Regulation of exit from mitosis in multinucleate *Ashbya gossypii* cells relies on a minimal network of genes

Mark R. Finlayson, A. Katrin Helfer-Hungerbühler, and Peter Philippsen
Department of Molecular Microbiology, Biozentrum, University of Basel, 4056 Basel, Switzerland

ABSTRACT **In *Saccharomyces cerevisiae*, mitosis is coupled to cell division by the action of the Cdc fourteen early anaphase release (FEAR) and mitotic exit network (MEN) regulatory networks, which mediate exit from mitosis by activation of the phosphatase Cdc14. The closely related filamentous ascomycete *Ashbya gossypii* provides a unique cellular setting to study the evolution of these networks. Within its multinucleate hyphae, nuclei are free to divide without the spatial and temporal constraints described for budding yeast. To investigate how this highly conserved system has adapted to these circumstances, we constructed a series of mutants lacking homologues of core components of MEN and FEAR and monitored phenomena such as progression through mitosis and Cdc14 activation. MEN homologues in *A. gossypii* were shown to have diverged from their anticipated role in Cdc14 release and exit from mitosis. We observed defects in septation, as well as a partial metaphase arrest, in *Agtem1*Δ, *Agcdc15*Δ, *Agdbf2/dbf20*Δ, and *Agmob1*Δ. *A. gossypii* homologues of the FEAR network, on the other hand, have a conserved and more pronounced role in regulation of the M/G1 transition. *Agcdc55*Δ mutants are unable to sequester AgCdc14 throughout interphase. We propose a reduced model of the networks described in yeast, with a low degree of functional redundancy, convenient for further investigations into these networks.**

Monitoring Editor
Rong Li
Stowers Institute

Received: Dec 23, 2010
Revised: Jun 23, 2011
Accepted: Jun 27, 2011

INTRODUCTION

Mitosis is coupled to different needs in different cell types. Requirements in most organisms, however, generally include correct positioning of the nucleus relative to the future cell division plane, and a variety of control mechanisms have been described that aid in ensuring correct orientation and timing of mitotic spindle elongation. One such control system is the large network of genes in *Saccharomyces cerevisiae* involved in mediating exit from mitosis, a cell cycle transition characterized by down-regulation of mitotic Clb2–cyclin-dependent kinase (Cdk) activity and resulting in events such as breakdown of the mitotic spindle, completion of cytokinesis, and chromosome decondensation (Bardin *et al.*, 2000). A single phosphatase called Cdc14 is pivotal to these steps in *S. cerevisiae*. Cdc14 not only mediates full reversal of Cdk activity, but it also has direct influence on specific aspects of mitosis such as rDNA segregation (Sullivan *et al.*, 2004) or spindle stabilization (summarized in Rock and Amon, 2009).

The regulation of Cdc14 is increasingly well understood (for recent reviews see Queralt and Uhlmann, 2008a; De Wulf *et al.*, 2009; Rock and Amon, 2009) and is based on localization control. During interphase, prophase, and metaphase, Cdc14 is sequestered in the nucleolus, where it is retained by association with its inhibitor, Net1 (Visintin *et al.*, 1999). During anaphase it is released throughout the nucleus as well as into the cytoplasm, where it is actively retained. This release occurs in two major phases and depends on the phosphorylation status of Net1.

The first phase of release is transient and brought about by the Cdc fourteen early anaphase release (FEAR) network (Stegmeier *et al.*, 2002). This initial wave of Cdc14 is crucial for some aspects of chromosome segregation, but it is not essential for cell cycle progression. Full stable release is only achieved upon the activation

This article was published online ahead of print in MBoC in Press (http://www.molbiolcell.org/cgi/doi/10.1091/mbc.E10-12-1006) on July 7, 2011.

Address correspondence to: Peter Philippsen (Peter.Philippsen@unibas.ch).

Abbreviation used: AFM, Ashbya full medium; *Ag*, *Ashbya gossypii*; ARS, autonomously replicating sequence; Cdk, cyclin-dependent kinase; FEAR, Cdc fourteen early anaphase release; MEN, mitotic exit network; *Sc*, *Saccharomyces cerevisiae*; SPB, spindle pole body; TL, time lapse.

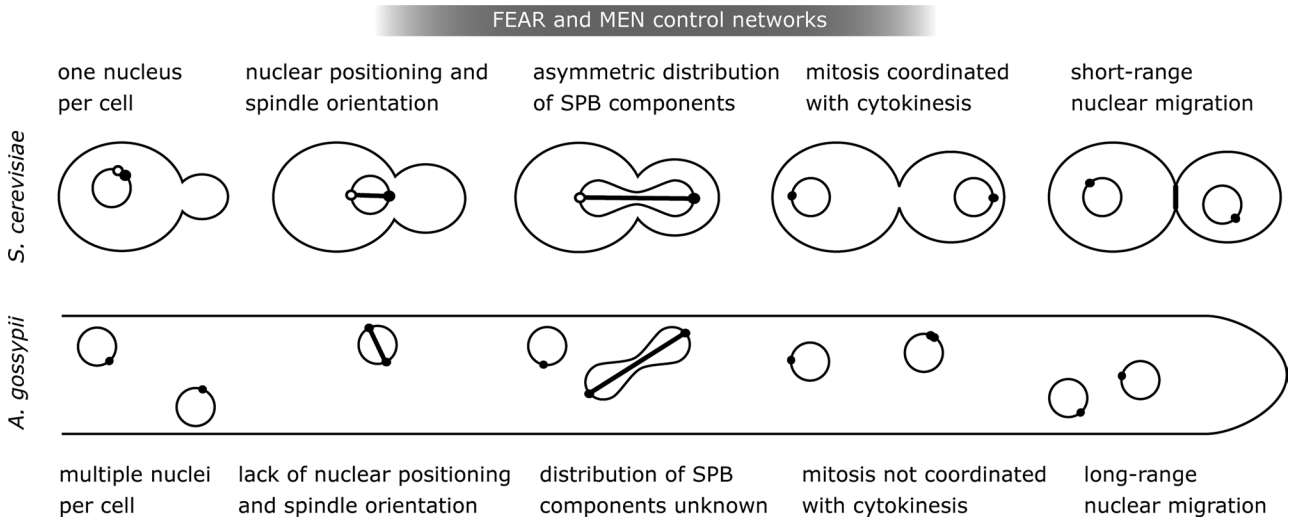

FIGURE 1: Nuclei in *S. cerevisiae* and *A. gossypii* are subject to entirely different cellular environments. Position of nuclei in *S. cerevisiae* is tightly controlled leading up to and during cell division. In *A. gossypii*, in which cell division does not take place, no such constraints exist, and nuclei divide asynchronously and without regard to orientation.

of the mitotic exit network (MEN), which is essential for mitotic exit. Whereas the FEAR network is primarily triggered by separase activation and is thus directly coupled to the metaphase/anaphase transition, the subsequently active MEN is proposed to rely on spatial cues or polarization along the division axis. It has been suggested that the MEN acts as a spatial control system linking correct orientation of the mitotic spindle to full Cdc14 release. Another possible role of the MEN is suggested to be in providing circuitry for various forms of signal modification (Bosl and Li, 2005). Positive feedback loops, for example, are believed to lead to the abruptness of changes needed during the final stages of mitosis (Holt *et al*., 2008). In addition, intrinsic oscillatory behavior observed for the Cdc14 phosphatase has been shown to depend on a functional MEN (Lu and Cross, 2010).

We wanted to know whether FEAR and MEN networks also function in multinucleated hyphae of the filamentous ascomycete *Ashbya gossypii*. For 95% of its genes, homologues are present in the genome of *S. cerevisiae*, the majority at syntenic positions (Dietrich *et al*., 2004). Despite this highly conserved genetic makeup, *A. gossypii* does not grow like budding yeasts but forms mycelia of multinucleate hyphae with altered nuclear cycle controls. Nuclei divide asynchronously in a common cytoplasm, are very motile even during mitoses, and are capable of bypassing each other while migrating long distances (Alberti-Segui *et al*., 2001; Gladfelter *et al*., 2006; Lang *et al*., 2010a). Consequently, nuclei are subject to much less temporal and orientational constraints when undergoing mitosis compared with *S. cerevisiae* (Figure 1). For instance, nuclei in *A. gossypii* can elongate with their spindle perpendicular to the growth axis. As anaphase progresses and comes into close proximity with the plasma membrane, the spindle turns into the direction of the growth axis. In addition, mitosis is not coupled to cytokinesis because septation only occurs every 40-80 µm, leading to syncytia containing roughly 8–12 nuclei (Wendland and Philippsen, 2000; Kaufmann and Philippsen, 2009). These seemingly less controlled nuclear cycles may have evolved after homologues of *S. cerevisiae* genes were lost. For example, *A. gossypii* carries homologues of all *S. cerevisiae* genes involved in septum formation but lacks two genes for septum degradation during cell separation, which explains why *A. gossypii* lacks cell separation (Kaufmann and Philippsen, 2009).

We study what role FEAR and MEN pathways play in this unique cellular environment and focus on the following question: Are such complex networks needed in this particular setting? If the advantages of the circuitry motifs that these components provide outweigh the roles in spatial control, then we would expect to observe functional conservation of large portions of the system.

RESULTS

A. gossypii Cdc14 is sequestered in the nucleolus during interphase and released during anaphase

The central phosphatase responsible for exit from mitosis in budding yeast, *S. cerevisiae* (*Sc*) Cdc14, was found to be highly conserved in *A. gossypii*, with an amino acid identity value of 77% predicted. *Sc*Cdc14 activity is heavily dependent on its localization. Many known subcellular sites of action have been described in *S. cerevisiae*, and we were interested in seeing whether localization patterns are conserved in *A. gossypii*. To this end we performed colocalization studies using *A. gossypii* (*Ag*) Cdc14–green fluorescent protein (GFP) and the nucleolar marker *Ag*Nop1-Cherry. Time-lapse imaging series revealed different phases of *Ag*Cdc14-GFP localization during the nuclear division cycle (Figure 2A): During interphase, *Ag*Cdc14 is sequestered within the nucleolus. The *Ag*Cdc14-GFP signal was shown to be restricted to within the area of *Ag*Nop1-mCherry, but also to have a granular localization pattern, seemingly composed of multiple foci (Figure 2A, 0′ 00″). During mitosis, *Ag*Cdc14 is then progressively released from this confined space and spreads to a total area of 3.8 µm^2 (Figure 2A, 2′ 30″), which indicates localization throughout the entire nucleoplasm. Coinciding with this release, *Ag*Cdc14 also localizes to two distinct foci (Figure 2A, 3′ 00″), which then migrate apart as mitosis progresses (Figure 2A, from 4′ 15″ on). After mitosis is complete, *Ag*Cdc14-GFP then relocalizes to the nucleoli (Figure 2A, 14′ 30″). As *Sc*Cdc14 was also described to localize to spindle pole bodies (SPBs) during anaphase in *S. cerevisiae* (Yoshida *et al.*, 2002), we hypothesized that this was also the case in *A. gossypii*. On this account, an *Ag*Cdc14-mCherry fusion was constructed and colocalized with *Ag*Tub4-YFP, an established component of the *A. gossypii* SPB (Lang *et al.*, 2010a). Single-plane imaging confirmed that *Ag*Cdc14-mCherry indeed localizes to SPBs in anaphase nuclei (Figure 2B). *Ag*Cdc14-GFP was also found to localize to developing

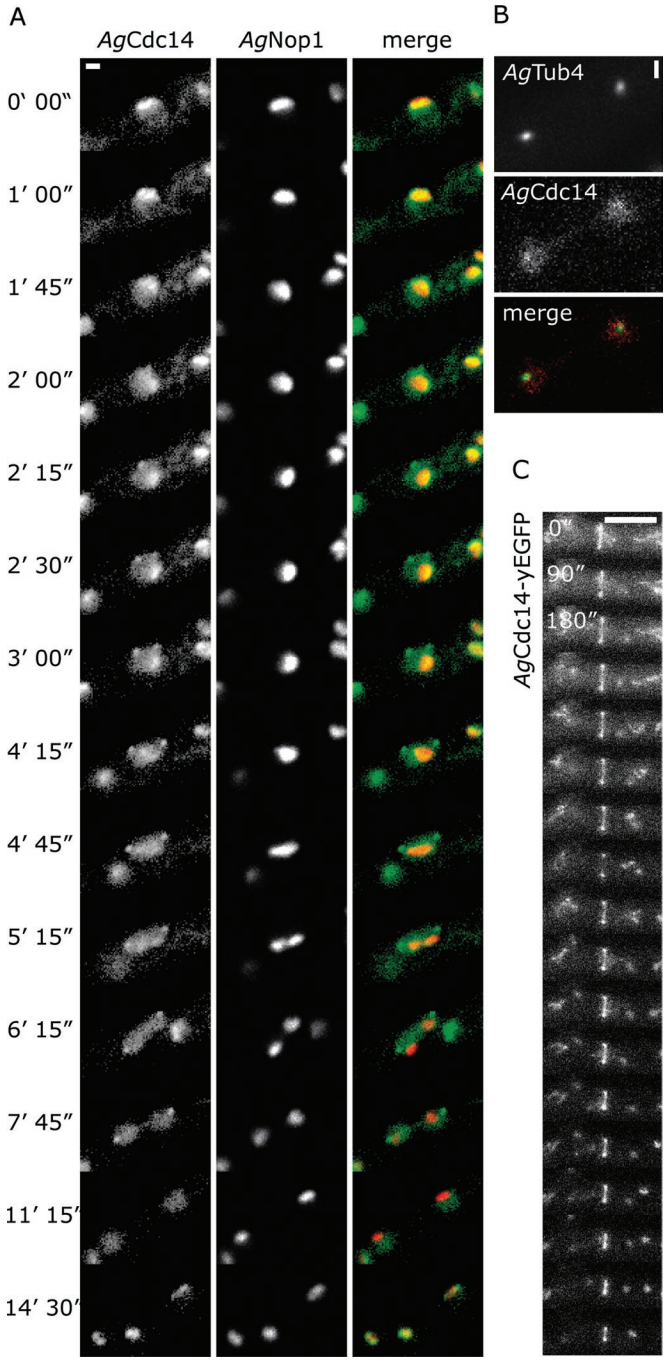

FIGURE 2: *Ag*Cdc14 localization. (A) Selection of time points showing the release and subsequent resequestration of *Ag*Cdc14-yEGFP from and into the nucleolus (visualized by *Ag*Nop1-mCherry) as a nucleus undergoes mitosis. Scale bar, 1 µm. (B) Still image from a time-lapse series tracking *Ag*Tub4-YFP and *Ag*Cdc14-yEGFP in a dividing nucleus. Only a single plane was captured in order to reduce the interval between channels to roughly 3 s. (C) Time-lapse series showing *Ag*Cdc14-yEGFP localization to septum of 20-h-old mycelium. Time interval, 3 min. Scale bar, 10 µm.

septa. In time-lapse series, protein levels did not appear to vary during ongoing septum constriction (Figure 2C). This septal localization suggests a pool of *Ag*Cdc14 present in the cytoplasm.

These results combined suggest that the basis of regulation of *Sc*Cdc14 appears to be conserved in *A. gossypii*, in that localization according to nuclear cycle stage seems to be central to function.

All MEN and FEAR components described in yeast are conserved on a sequence level in *A. gossypii*

The observed release patterns suggesting a conserved form of regulation led to investigations concerning the underlying regulatory pathways. Do these networks also exist in *A. gossypii*? Orthologues for all genes proposed to be involved in MEN and FEAR signaling in *S. cerevisiae* were found to be annotated in the *A. gossypii* genome (Dietrich *et al.*, 2004). All orthologues are syntenic, and all domains predicted for MEN component in *S. cerevisiae* were also predicted for the *A. gossypii* orthologues (Supplemental Figure S1). Computed amino acid identity values range between 19% for the SPB anchor (Lang *et al.*, 2010b) *Ag*Nud1 and 89% for the putative PP2A phosphatase subunit *Ag*Pph21 (Table 1).

MEN homologue localization is analogous to that in *S. cerevisiae*

Given the sequence level conservation of the *S. cerevisiae* MEN pathway in *A. gossypii*, we were interested to see whether functionality was also conserved. To study the aspect of localization, we constructed C-terminal yeast-enhanced green fluorescent protein (yEGFP) fusions for the putative GTPase *Ag*Tem1 and guanine nucleotide exchange factor *Ag*Lte1.

*Ag*Tem1-yEGFP was shown to localize to distinct foci, reminiscent of the localization of *Sc*Tem1 to SPBs (Bardin *et al.*, 2000) in *S. cerevisiae* (Figure 3A). To validate this, we performed an immunofluorescence staining using antibodies against *Ag*Tub1 and were able to demonstrate colocalization of *Ag*Tem1-yEGFP with the microtubule organizing centers (Figure 3B).

In time-lapse recordings of growing hyphae, by studying their movement for up to ½ h, we were able to identify *Ag*Tem1-yEGFP foci of dividing nuclei (Figure 3A, yellow arrowhead) and follow them through the course of mitosis. We were interested to see whether asymmetric, polar localization of *Ag*Tem1-yEGFP occurred at any stage of the nuclear division cycle, as is the case in *S. cerevisiae*. This was shown not to be the case (Figure 3C). *Ag*Tem1-yEGFP was distributed to both foci evenly, with no loss or gain of signal intensity over time.

*Ag*Lte1-yEGFP also exhibited a localization pattern analogous to that of its *S. cerevisiae* orthologue (Seshan *et al.*, 2002). Observing young mycelia up to 20 h in age, we could see a strong localization of *Ag*Lte1-yEGFP to the hyphal tip, with the signal strength declining toward the back but sometimes still visible up to 10 mm from the tip (Figure 3D). The signal intensity was not the same at different branches of the same mycelium, sometimes missing entirely. In single-plane images, localization to the outer, cortical zone of the hyphal tip was observed (Figure 3E).

These analogous localization patterns of *Ag*Lte1 and *Ag*Tem1, combined with the high sequence identity of core MEN orthologues, hint at the possibility of an analogous cellular function of MEN components in *A. gossypii*.

MEN homologue null mutants are viable but are defective in septation

To clarify whether the *A. gossypii* orthologues of this pathway fulfill similar roles, we created single-gene deletions for *Ag*TEM1, *Ag*CDC15, *Ag*DBF2/DBF20, *Ag*MOB1, *Ag*LTE1, *Ag*KIN4/FRK1, and *Ag*KEL1/KEL2. Unexpectedly, viable null mutants could be generated for all selected MEN-related orthologues in *A. gossypii*. In growth assays at the optimal temperature of 30°C, all strains exhibited radial growth speeds similar to wild type (WT), except *Agkin4/frk1*Δ and *Agkel1/kel2*Δ mutants, which (expressed as radial colony growth speed) grew ~10% more

	A. gossypii orthologue		*S. cerevisiae* 1st orthologue				*S. cerevisiae* 2nd orthologue		
Common	Systematic	aa	Systematic	aa	ID	Null mutant	Common	Systematic	aa
*Sc*CDC14	AEL025W	537	YFR028C	551	77%	Lethal			
*Sc*NET1	AAL181C	1222	YJL076W	1189	30%	Double: viable	*Sc*TOF2	YKR010C	771
*Sc*BFA1	ACL090C	474	YJR053W	574	34%	Viable			
*Sc*BUB2	ADR131C	305	YMR055C	306	76%	Viable			
*Sc*CDC15	AER223C	903	YAR019C	974	43%	Lethal			
*Sc*CDC5	ACL006W	709	YMR001C	705	79%	Lethal			
*Sc*DBF2	ADR033W	578	YGR092W	572	79%	Double: lethal	*Sc*DBF20	YPR111W	564
*Sc*KEL1	ADL149W	1211	YHR158C	1165	43%	Double: viable	*Sc*KEL2	YGR238C	883
*Sc*KIN4	ACR119W	932	YOR233W	865	38%	Viable*	*Sc*FRK1	YPL141C	866
*Sc*LTE1	ACR292W	1439	YAL024C	1435	46%	Lethal at low temperature			
*Sc*MOB1	ADL236W	296	YIL106W	314	72%	Lethal			
*Sc*NUD1	ADR416W	757	YOR373W	852	19%	Lethal			
*Sc*TEM1	AER132W	233	YML064C	245	72%	Lethal			
*Sc*CDC55	AFR195W	455	YGL190C	526	78%	Viable			
*Sc*ESP1	AAR089C	1618	YGR098C	1631	50%	Lethal			
*Sc*FOB1	AGR086C	534	YDR110W	567	39%	Viable			
*Sc*PDS1	AGR083W	295	YDR113C	374	32%	Lethal			
*Sc*PPH21	ADR099C	362	YDL134C	370	89%	Double: viable	*Sc*PPH22	YDL188C	378
*Sc*SLK19	AGR229W	705	YOR195W	822	24%	Viable			
*Sc*SPO12	ADL140C	173	YHR152W	174	22%	Double: viable	*Sc*BNS1	YGR230W	137
*Sc*TPD3	ACR279C	603	YAL016W	636	78%	Viable			
*Sc*ZDS1	AAL185W	1018	YMR273C	916	34%	Double: viable	*Sc*ZDS2	YML109W	943

aa, length in amino acids; ID, calculated sequence identity.
*Double deletion N/A.

TABLE 1: Homologues of genes involved in exit from mitosis.

slowly (Figure 4A). Mild growth impairments could be observed in all mutants at nonoptimal temperatures, notably including an increased sensitivity to low temperatures in *Aglte1*Δ mycelia. The discovery that deletion mutants of MEN homologues in *A. gossypii* are viable and grow at WT-like speeds on plates is in contrast to the situation in budding yeast, where MEN signaling is essential.

Isolation of spores from mature mycelia revealed severe sporulation deficiencies in *Agtem1*Δ, *Agcdc15*Δ, *Agdbf2/dbf20*Δ , and *Agmob1*Δ mutants (Figure 4B). To trigger the sporulation program at a younger developmental stage (allowing microscopy with small mycelia), we transferred 1-d-old mycelia to nutrient-deprived medium. Differences between WT and *Agtem1*Δ samples could be observed within 48 h of switching to low nutrient levels: sporangia (bloated compartments along the hyphae) in mutant strains did not develop properly. We observed clear defects in septation in our mutants that did not display the regular segmentation of the hyphae needed for proper spore formation (Figure 4C). Strongly reduced numbers of spores started forming after 72 h within noncompartmentalized sections of the hyphae (Figure 4C). The lack of septa could be readily visualized in all our MEN homologue strains by using calcofluor white to stain chitin, which is enriched at septation sites. We performed this experiment on all mutants and additionally included a *Agbub2*Δ strain. *Sc*Bub2 has been described as the GTPase-activating protein of *Sc*Tem1 in *S. cerevisiae* (Pereira *et al.*, 2000), and it was hypothesized that a lack of *Ag*Bub2 may lead to an increase in *Ag*Tem1 activity if the pathway is conserved. *Agtem1*Δ, *Agcdc15*Δ, *Agdbf2/dbf20*Δ, and *Agmob1*Δ strains all displayed low counts of septa along growing hyphae, whereas our *Agbub2*Δ strain showed a slight increase in numbers (Figure 4D). On more detailed inspection, we found that septa were not occurring more frequently along mature hyphae (Figure 4E, left) in this strain. Instead, septa were maturating faster: Chitin rings could be found closer to the tip than in wild type (Figure 4E, middle and right).

In agreement with this apparent role in septation, *S. cerevisiae* MEN components have been shown to localize to the bud neck; more specifically, *Sc*Tem1, *Sc*Cdc15, *Sc*Dbf20, and *Sc*Dbf2 have been shown to be important for cytokinesis (Meitinger *et al.*, 2010) and control of the repolarization of the actin cytoskeleton (Corbett *et al.*, 2006). What stood out in our experiments was a consistent sporulation phenotype across all MEN homologue strains. This can be understood as an indication that the core signaling cascade as described in budding yeast may be intact in *A. gossypii*.

MEN homologue null mutants show partial arrest in metaphase but no defects in M-to-G1 transition

To investigate whether MEN homologues in *A. gossypii* fulfill a function in nuclear cycle progression, we deleted *Ag*TEM1, *Ag*CDC15, *Ag*DBF2/DBF20, and *Ag*LTE1 in an *Ag*H4-GFP *Ag*Tub4–yellow fluorescent protein (YFP) background. We were thus able to

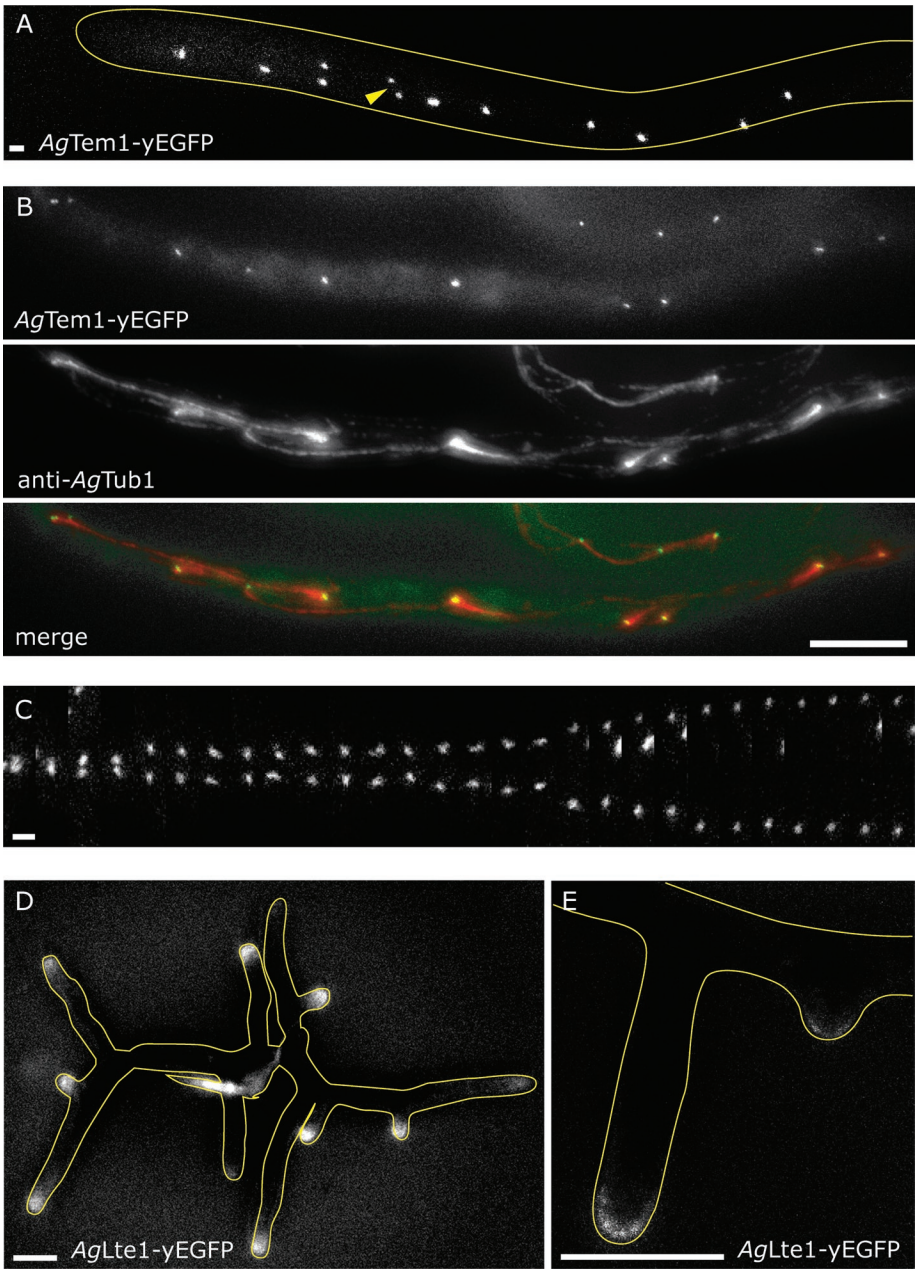

FIGURE 3: *Ag*Tem1 and *Ag*Lte1 localization. (A) Still image from time-lapse series tracking *Ag*Tem1-yEGFP in growing hyphae. Arrowhead indicates nucleus chosen for montage in C. Projection of 11 Z-planes, 0.5 µm apart. Scale bar, 1 µm. (B) Colocalization study of *Ag*Tem1-yEGFP (top) and *Ag*Tub1 (middle). Scale bar, 10 µm. (C) Montage of nucleus undergoing mitosis. Time interval, 1 min. (D) *Ag*Lte1-yEGFP in 20-h-old mycelium. Maximum intensity projection of five planes with Z-distance of 1 µm. (E) *Ag*Lte1-yEGFP in 22-h-old mycelium. Single plane. Scale bar, 10 µm.

differentiate whether individual nuclei were in interphase, metaphase, or anaphase, and inspected more than 300 nuclei for each strain, only taking into consideration fast-growing hyphae that had recently undergone tip splitting and thus were growing at maximum speed. MEN orthologue mutants *Agtem1*Δ, *Agcdc15*Δ, and *Agdbf2/dbf20*Δ were shown to have an enrichment of metaphase nuclei (Figure 5A). *Aglte1*Δ showed no increase of metaphase nuclei within propagating hyphae. To investigate the possibility of any spatial dependence of these observations, we measured the position of nuclei identified as being in metaphase in selected mutants relative to the hyphal tip. No significant increase or decrease of metaphase nuclei was detected toward the tip in the measured strains *Agtem1*Δ and *Aglte1*Δ (Figure 5B).

This investigation of nuclear stages in *A. gossypii* MEN homologue mutants reveals great differences compared with MEN mutants in *S. cerevisiae*. The data suggest a major deviation from the role established in budding yeast, in which MEN temperature-sensitive mutants arrest at the M/G1 transition. The partial arrest in metaphase discovered in the *Agtem1*Δ, *Agcdc15*Δ, *Agdbf2/dbf20*Δ , and *Agmob1*Δ strains (with identical phenotypes once again suggesting that the core kinase cascade of the pathway is conserved) is surprising insofar as it suggests a crucial role of these MEN signaling cascade homologues prior to anaphase, which represents a novel finding for eukaryotes.

*Ag*Cdc14 release dynamics is unaffected in MEN homologue *Ag*CDC15 null mutant

Given that an immediate consequence of MEN signaling in *S. cerevisiae* is sustained release of *Sc*Cdc14 during later stages of anaphase, experiments were conducted to clarify the role of the *A. gossypii* orthologues in localization patterns of *Ag*Cdc14. To be able to detect minor changes in release dynamics, we introduced *Ag*Pds1-mCherry into an *Ag*Cdc14-GFP background strain. *Sc*Pds1, or securin, is an inhibitor of separase and is degraded in an anaphase-promoting complex–dependent manner, triggering the onset of anaphase (Cohen-Fix *et al.*, 1996). The intention of including this marker was to provide an additional visual cue (the disappearance of *Ag*Pds1-Cherry) for the metaphase/anaphase transition as a temporal reference on which to base the timings of our observations of *Ag*Cdc14-yEGFP. The open reading frame (ORF) of *Ag*CDC15 was deleted in this strain, and time-lapse image series of both mCherry and GFP signals were acquired (Figure 6B). *Ag*Cdc14 dynamics was shown to be very similar to what was observed in wild type. Seemingly coincidental with the first signs of *Ag*Pds1 degradation, *Ag*Cdc14 would start to become visible at the SPBs, indicating initial release from the nucleolus. Around the time *Ag*Pds1 reached baseline levels, *Ag*Cdc14 release was to full extent. No return of *Ag*Pds1 could be made out in postmitotic nuclei, where *Ag*Cdc14 was resequestered in the nucleoli. To provide quantitative data, we measured various features of these dividing nuclei (full description in *Materials and Methods*). To quantify sequestered Cdc14, we calculated the number of high-intensity yEGFP-channel pixels within fixed mitotic areas (Figure 6B, bottom, yellow polygon). For *Ag*Pds1 levels, we measured mCherry signals at the center of nuclei (Figure 6B, middle, circular area). We also measured elongation of the mitotic spindle using the SPB foci of *Ag*Cdc14, which were visible for the

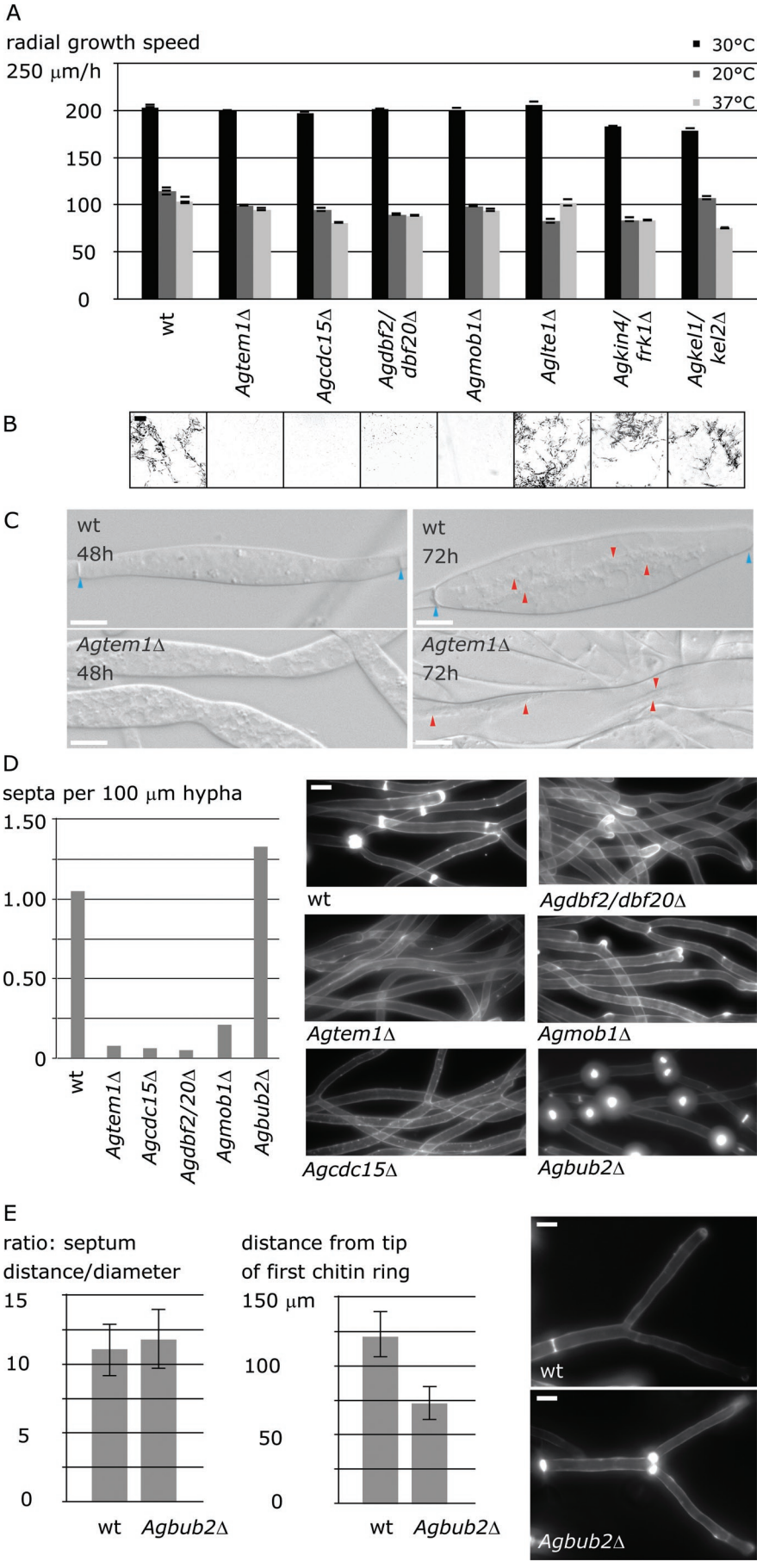

entire duration of anaphase. The measurements confirmed our prior observations (Figure 6A). No significant differences were found between *Agcdc15Δ* and wild-type nuclei concerning the timing and sequence of such events as *Ag*Pds1 degradation, *Ag*Cdc14 release, spindle elongation, or *Ag*Cdc14 resequestration.

The lack of a role in *Ag*Cdc14 release for the MEN homologue *Ag*Cdc15 minimizes the possibility that the partial metaphase arrest observed in MEN homologue mutants is mediated via downstream *Ag*Cdc14 and likely marks a decoupling of the conserved signaling cascade from this important regulatory function first described in budding yeast. This does not rule out a regulatory function toward *cytoplasmic Ag*Cdc14. The experiment also provided further important information on the nature of the partial metaphase arrest seen in MEN homologue mutants in terms of time of action. The function involved in the partial arrest clearly precedes *Ag*Pds1 degradation, as no delay in spindle elongation was observed in nuclei in which *Ag*Pds1 degradation was successfully triggered.

*Ag*Cdc14 is permanently released in FEAR homologue *Ag*Cdc55 null mutant

The discovery that MEN homologues in *A. gossypii* do not contribute to *Ag*Cdc14 release or

FIGURE 4: MEN homologue mutant phenotypes. (A) Radial growth speeds of mutants at 30, 20, and 37°C after 5 d. Values represent the mean of two or three separate measurements done with individual strains, which are indicated by thin horizontal bars. (B) Samples taken from spore preparations of inner 3 cm of 6-d-old colonies. Scale bar, 0.1 mm. (C) DIC images of hyphae after 48 and 72 h in 1:4 diluted Ashbya full medium (AFM) liquid cultures. Blue arrowheads indicate mature septa. Red arrowheads indicate developing spores. Scale bar, 10 μm. (D) Septum counts along randomly selected hyphae of varying developmental stage (left). Right, examples of calcofluor white stainings visualizing chitin-harboring septa performed on hyphae taken from liquid AFM cultures inoculated with pieces of mycelium from edges of plate colonies. Chitin stains are visible at growing and emerging hyphal tips, as well as at septa. Scale bar, 10 μm. (E) Detailed analysis of septum distribution in *Ag*bub2Δ. Left, mean and SD of the ratio of the distance between septa to the width of septa. Width was taken into account because of an observed positive correlation of hyphal diameter and growth speed. The graph can thus be regarded as a representation of the distance between neighboring septa, corrected for this growth speed bias. Middle, mean and SD of the distance measured from the growth tip to the first complete chitin ring. Right, examples of calcofluor white stainings used for tip distance measurements. Scale bar, 10 μm.

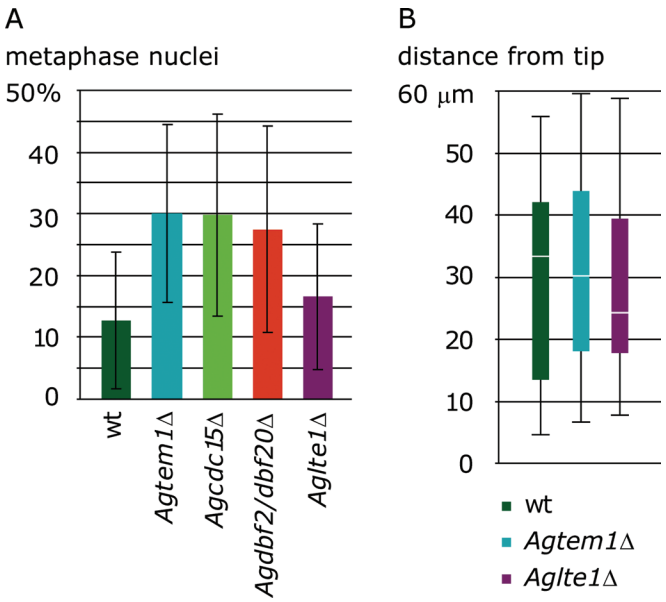

FIGURE 5: Occurrence of metaphase nuclei in MEN mutants. (A) Percentages of nuclei within individual hyphae found to be in metaphase in wild-type reference strain (*Ag*H4-GFP *Ag*Tub4-YFP) and MEN mutants. Error bars represent one SD. A graph of total stage counts across all hyphae is provided in Supplemental Figure S3. (B) Mean distance of metaphase nuclei from the hyphal tip. Whisker plot depicts 25th percentiles.

M-to-G1 transition raises the question of whether the entire underlying regulatory machinery known from *S. cerevisiae* is uncoupled from these tasks or whether control over *Ag*Cdc14 activation has perhaps been bestowed on a reduced network made up of homologues of the FEAR pathway.

A first deletion experiment revealed that the putative FEAR orthologue *Ag*Cdc55 was essential for the viability of young mycelia, as *Agcdc55*Δ mutants ceased growth and lysed after ~24 h. We deleted the *Ag*CDC55 ORF in a *Ag*Cdc14-yEGFP background strain and assessed GFP localization prior to lysis of the cells. In *Agcdc55*Δ, the *Ag*Cdc14-yEGFP localization pattern was at all times and in all nuclei reminiscent of the unsequestered signals we observed for anaphase nuclei in wild type: *Ag*Cdc14-yEGFP exhibited a low-intensity signal throughout the nucleoplasm and bright foci at the SPBs (Figure 7A). It appears that *Ag*Cdc14-yEGFP is constantly in a released state in these mutants. The number of nuclei is also strongly reduced in these mutants compared with wild-type cells, suggesting difficulties in progression through mitosis. Of all nuclei observed, almost all appeared to be in interphase, and only one instance of mitosis was captured by imaging (Figure 7B). In this instance, it seemed that anaphase spindle elongation was not affected (in terms of duration and attained length), although it was not clear, due to lack of movement, whether the nuclei could properly separate after maximum elongation was reached. In the mutant strain, nuclei were also observed to be much larger than in wild type, with diameters of more than 5 μm measured in most cases, compared with 2 μm for wild-type.

The observation represents a strong contrast to *S. cerevisiae*, in which *Sccdc55*Δ cells show premature release of *Sc*Cdc14 but successful, albeit delayed, return to the nucleolus (Queralt *et al.*, 2006).

*Agspo12*Δ mutants show nuclear segregation defects

The phenotype of *Agcdc55*Δ was not the only large difference in severity found for putative FEAR homologues compared with *S. cerevisiae*. Another striking outcome was observed in *Agspo12/bns1*Δ mutants (for *Sc*Spo12, see Stegmeier *et al.* [2002]). We deleted the *Ag*SPO12/BNS1 ORF in a *Ag*H4-GFP background in order to monitor nuclear behavior. Mutants would often cease growth at the germ bubble stage and occasionally could form primary germ tubes. In such cells we were able to monitor nuclei over a period of up to 14 h (Figure 8A). Nuclei were in motion during the entire duration of the experiment, but mitosis was strongly impaired, as shown by time-lapse imaging. The following describes the behavior of the nucleus indicated by the arrowhead. The beginning and end of mitosis could not be identified, and DNA was seemingly separated in multiple attempts over the course of ~4–5 h (for comparison, this normally takes no longer than 15 min in wild-type cells, as shown in Figure 8B). In first step, only part of the DNA is moved, creating two fractions with differing signal intensities. In a second step, taking roughly 2 h, more DNA is transferred, resulting in two equally bright nuclei.

Given the putative role as an inducer of *Ag*Cdc14 activation, the apparent failure to undergo nuclear abscission in these cells may stem from failed release of the phosphatase. To investigate sequestration specifically, we additionally constructed a *Agspo12/bns1*Δ strain carrying *Ag*Cdc14-yEGFP and could only see the phosphatase in its sequestered form. Unfortunately, however, these cells displayed even less viability than *Agspo12/bns1*Δ H4-GFP cells, with no germ tubes forming at all and no mitotic events successfully recorded. This may hint at compromised functionality of our *Ag*Cdc14-yEGFP construct.

Other FEAR homologues

Mitotic stage counts as performed in the MEN orthologue mutants were not possible in *Agslk19*Δ. On inspection of *Ag*Tub4-YFP in the strains generated for the experiment, it became apparent that the nuclei in these mutants could not be categorized in a manner comparable to the data collected previously. Nuclei (*Ag*H4-GFP patches) could often be observed that had three (Figure 9A, red arrowhead) or no SPBs (Figure 9A, yellow arrowhead). In addition, there seemed to be detached SPBs within the cytoplasm, not stably connected to any nuclei at all, or connected to what appeared to be fragments of nuclei (Figure 9A, blue arrowheads). We also noticed morphological abnormalities of nuclei in the form of aberrant shapes of *Ag*H4-GFP. In addition, density of nuclei was roughly half of that of wild-type cells, reflecting a decrease in frequency of mitosis.

To investigate whether the decreased mitotic activity detected in *Agslk19*Δ was caused by compromised *Ag*Cdc14 regulation, we repeated the deletion in *Ag*Cdc14-yEGFP cells. *Ag*Cdc14-yEGFP sequestration and release seemed intact, with typical wild-type like localization patterns throughout anaphase (Figure 9B).

Mitotic stage counts were possible for *Agfob1*Δ and *Agzds1/zds2* mutants. Quantifications showed that no significant enrichment of any stage of the nuclear division cycle could be detected in these strains (Figure 9C). Percentage values of metaphase nuclei were 12.7 ± 11.1% (1 SD, N = 358) for wild type, 12.7 ± 9.9% (1 SD, N = 347) for *Agfob1*Δ, and 8.5 ± 7.0% (1 SD, N = 221) for *Agzds1/zds2*Δ.

*Agzds1/zds2*Δ cells also have no apparent trouble proceeding through mitosis. *Ag*Cdc14-yEGFP sequestration and release were also shown to occur in this strain (Figure 9D). We had expected a phenotype in nuclear division cycle progression since the *Agcdc55*Δ mutant shows such clear malfunctioning and *Ag*Zds1/Zds2 is a potential upstream inhibitor of the PP2A, judging by its function in *S. cerevisiae* (Queralt and Uhlmann, 2008b).

The lack of mitotic or developmental phenotype in *Agfob1*Δ mutants is actually similar to *S. cerevisiae*, in which *Sc*Fob1 deletion shows no phenotype in synchronized cells (Stegmeier *et al.*, 2004).

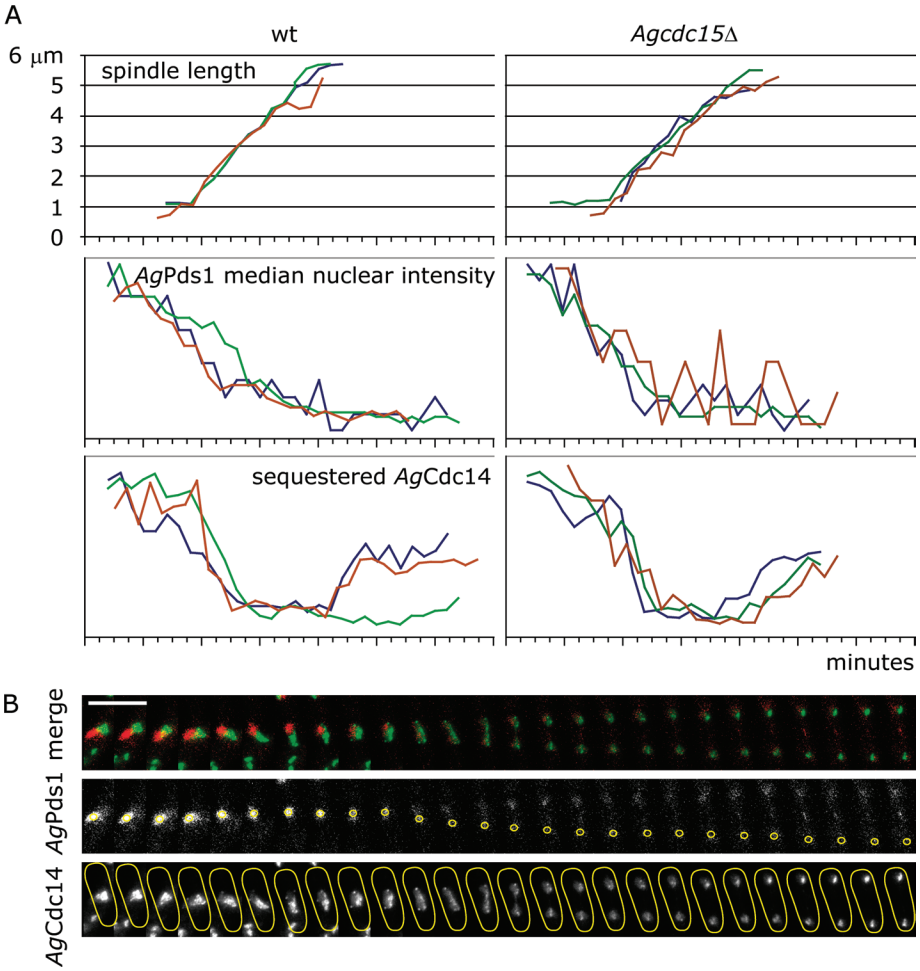

FIGURE 6: Dynamics of *Ag*Cdc14 release in *Agcdc15*Δ mutant. Measurement details in *Materials and Methods* section. Different colors indicate individual experiments. Overlay of measurements by translation along the *x*-axis (synchronization of data between experiments) and scaling along the *y*-axis (mapping to comparable ranges). Spindle lengths (top) were not scaled vertically, and so units (μm) were retained. Other (signal intensity) measurements are in arbitrary units due to scaling. (B) Time-lapse series of *Agcdc15*Δ *Ag*Cdc14-GFP *Ag*Pds1-mCherry nucleus undergoing mitosis as used for measurements. Yellow polygons demonstrate areas measured to generate data shown in Figure 7. Time interval, 1 min. Scale bar, 10 μm.

Possibly, *Ag*Fob1 also only has a minor role as in *Ag*Cdc14 regulation, which, as in budding yeast, only becomes apparent when cell cycle progression is perturbed.

DISCUSSION

Major deviation of MEN homologue pathway from role in budding yeast

Homologues of the MEN likely function together as a GTPase-coupled kinase cascade at the SPBs in *A. gossypii*. *Ag*Tem1, *Ag*Cdc15, *Ag*Mob1, and *Ag*Dbf2/Dbf20 mutants all share common phenotypes, indicating a conserved signaling unit. *Ag*Lte1 is likely to play no role within this signaling cascade, as no similar effects could be detected in knock-out mutants. *Ag*Bub2 possibly has a conserved function as a negative regulator of the signaling cascade. This functional unit seems to be uncoupled from any function in *Ag*Cdc14 release and exiting mitosis. No arrest in anaphase could be detected and no defects in timely *Ag*Cdc14 release could be observed upon obstruction of the signaling network.

Of interest, however, these MEN homologues appear to play a crucial role in passage through M phase. The time point of action is clearly prior to initiation of anaphase, as no change in nuclear division dynamics could be made out upon onset of *Ag*Pds1 disappearance. Within the *S. cerevisiae* nucleus, the spindle assembly checkpoint inhibits the degradation of Pds1 by complexing Cdc20 until kinetochores are properly attached to microtubules. Perhaps a similar system exists in *A. gossypii* involving MEN homologues promoting anaphase upon sufficient formation of cytoplasmic microtubules at the outer plaque of mitotic SPBs.

In any case, the effect on mitosis observed was not dependent on the position of the nuclei within the hypha. Given the symmetrical localization of *Ag*Tem1 to both SPBs after their duplication, nuclei probably also lack any basis for sensing of hyphal polarity. Most likely, for nuclei to be able to differentiate between sister SPBs, steeper gradients than observed for *Ag*Lte1 would be needed in order to be detected. Such gradients rely on structures like the bud neck in *S. cerevisiae* to provide sharp transitions across short distances. It is likely that *Ag*Lte1 plays a role in cell polarity; however, it appears that this polarity is not inherited by the nuclei.

*Ag*Cdc14 release was not affected in MEN homologue mutants. This uncoupling of the MEN from *Ag*Cdc14 sequestration control, however, does not rule out a function in cytoplasmic regulation, as has been described for *Sc*Dbf2 (Mohl *et al.*, 2009).

It is actually quite likely that, as in *S. cerevisiae*, MEN homologues are responsible for the retention of *Ag*Cdc14 in the cytoplasm, allowing its localization to the septation sites, where it promotes or enables septum development and maturation. Having an SPB-bound activator of septation would lead to the quicker closing of septa in regions containing many nuclei. This may contribute to a more equal distribution of nuclei among sporangia in mature hyphae.

Perhaps a defect in cytoplasmic retention in MEN mutants eventually leads to increased levels of *Ag*Cdc14 within the nucleus, which would go hand in hand with decreased Cdk activity. This might help to explain the metaphase delay exhibited.

FEAR homologue functions are conserved to various degrees

Our experiments indicate that control over *Ag*Cdc14 activation in *A. gossypii* has been bestowed on a network made up of homologues of the FEAR pathway. Deletion of *Ag*CDC55 was lethal and *Ag*Cdc14 was permanently released. This stands in contrast to *Sccdc55*Δ cells, which show premature release of *Sc*Cdc14 but successful, albeit delayed, return to the nucleolus. This discrepancy suggests that in *A. gossypii*, *Ag*Cdc55 down-regulation might be entirely sufficient for full, sustained release and thus may belong to a reduced set of genes causing *Ag*Cdc14 activation, as opposed to a more complex system with functional overlap of multiple components each with partial or nonessential contributions. The inability to resequester *Ag*Cdc14 during interphase hints that $PP2A^{AgCdc55}$ may

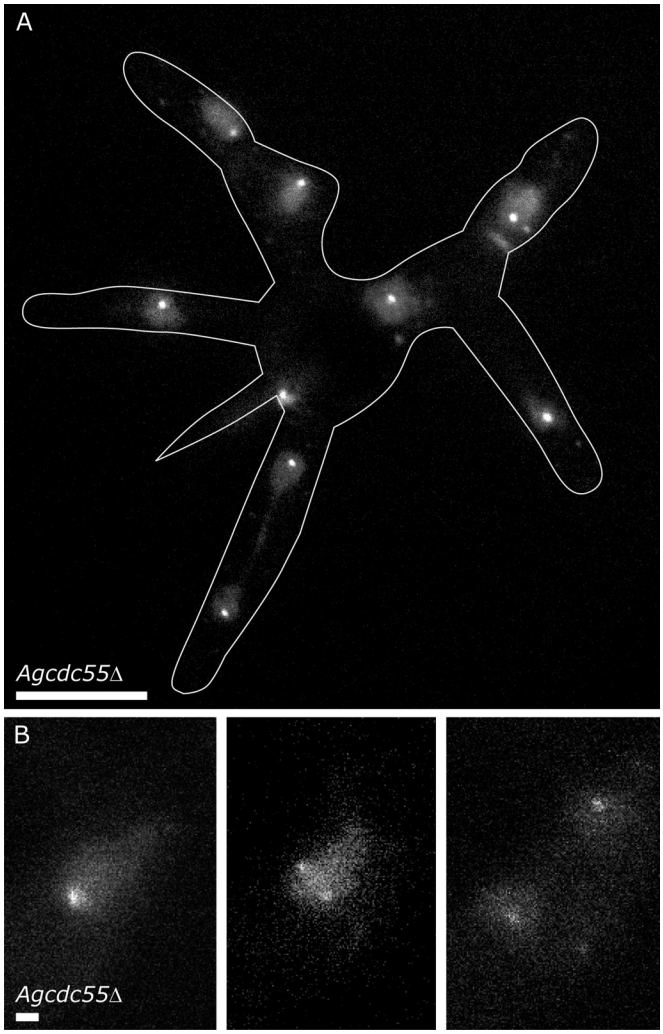

FIGURE 7: *Ag*Cdc14 release in *Agcdc55*Δ mutant. (A) *Ag*Cdc14-yEGFP signal in 18-h-old *Agcdc55*Δ mycelium. Maximum-intensity projection of 11 planes with a Z-distance of 0.5 µm. Scale bar, 10 µm. (B) *Ag*Cdc14-yEGFP signal in dividing nucleus of 20-h-old *Agcdc55*Δ mycelium. Images taken 17 and 18 min apart, respectively. Scale bar, 1 µm.

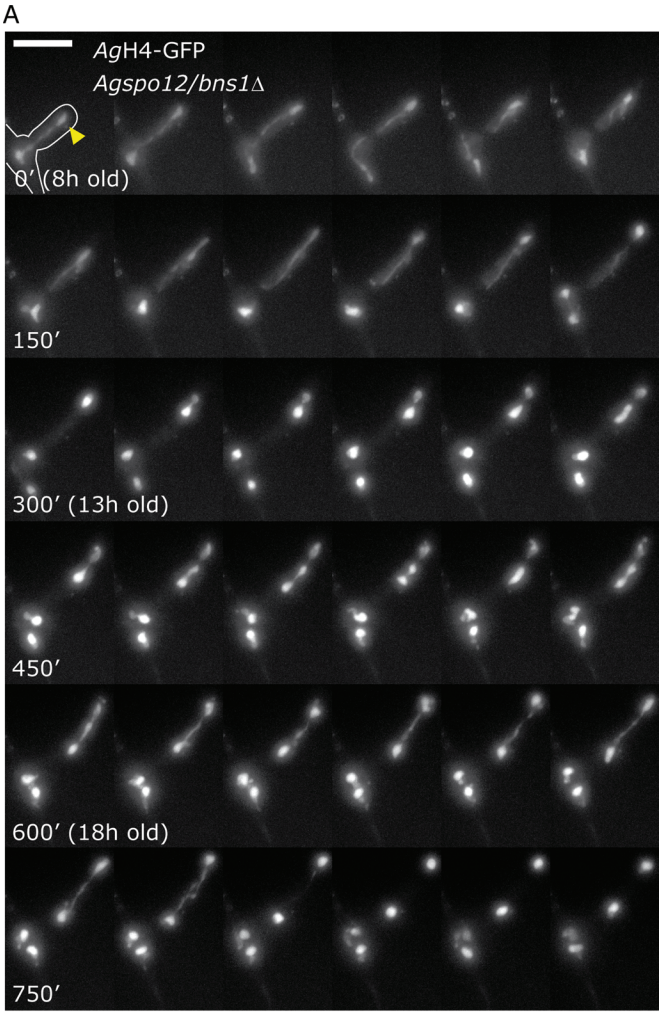

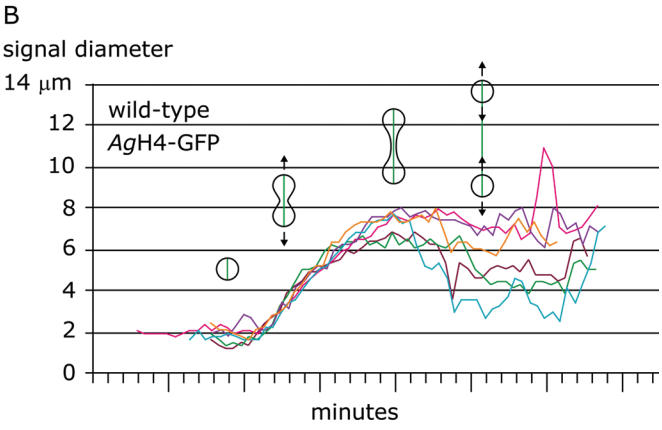

FIGURE 8: *Agspo12/bns1*Δ mutant. (A) Time-lapse series of *Ag*H4-GFP in *Agspo12/bns1*Δ germling. Time interval, 25 min, beginning at 8 h after spreading of spores. Scale bar, 10 µm. (B) Anaphase dynamics of wild-type nuclei for comparison. Overlay of multiple measurements of *Ag*H4-GFP signal diameter of mitotic nuclei in wild-type reference strain.

be the sole phosphatase involved in dephosphorylation of *Ag*Net1 in *A. gossypii*. In *S. cerevisiae*, Cdc14 itself is believed to contribute to this task.

One possible explanation for the growth defects and oversized nuclei of *Agcdc55*Δ could be the continuous reversal of S-phase Cdk activity by a perpetually active AgCdc14, since FEAR release of Cdc14 has been shown to be crucial in the termination of Clb5-Cdk activity (Jin *et al.*, 2008). One consequence of weakened S-phase Cdk activity could potentially be the misregulation of DNA replication.

Spo12 is a further case in which deletion causes more severe disturbances in *A. gossypii* than in *S. cerevisiae*. In the H4-GFP background strain, *Agspo12*Δ mutants displayed severe difficulties in nuclear division. The phosphorylation site S118 in Spo12 of *S. cerevisiae*, which is essential for function within FEAR (Tomson *et al.*, 2009), is conserved in *A. gossypii*, which speaks in favor of a conserved role in *Ag*Cdc14 regulation. The behavior exhibited by nuclei in mutants may reflect problems in rDNA segregation. As mentioned in the case of *Agcdc55*Δ, a loss of AgCdc14 activity may also postpone the termination of *Ag*Clb5/Clb6 Cdk, leaving many S-phase Cdk substrates phosphorylated. Unfortunately, *Ag*Cdc14 dynamics in *Agspo12*Δ cells could not be determined due to reduced viability of *Agspo12*Δ deletions specifically in *Ag*Cdc14 background strains.

The *Agzds1/zds2*Δ deletion poses an unexpected result. Concerning a possible function in FEAR, we anticipated at least a mild

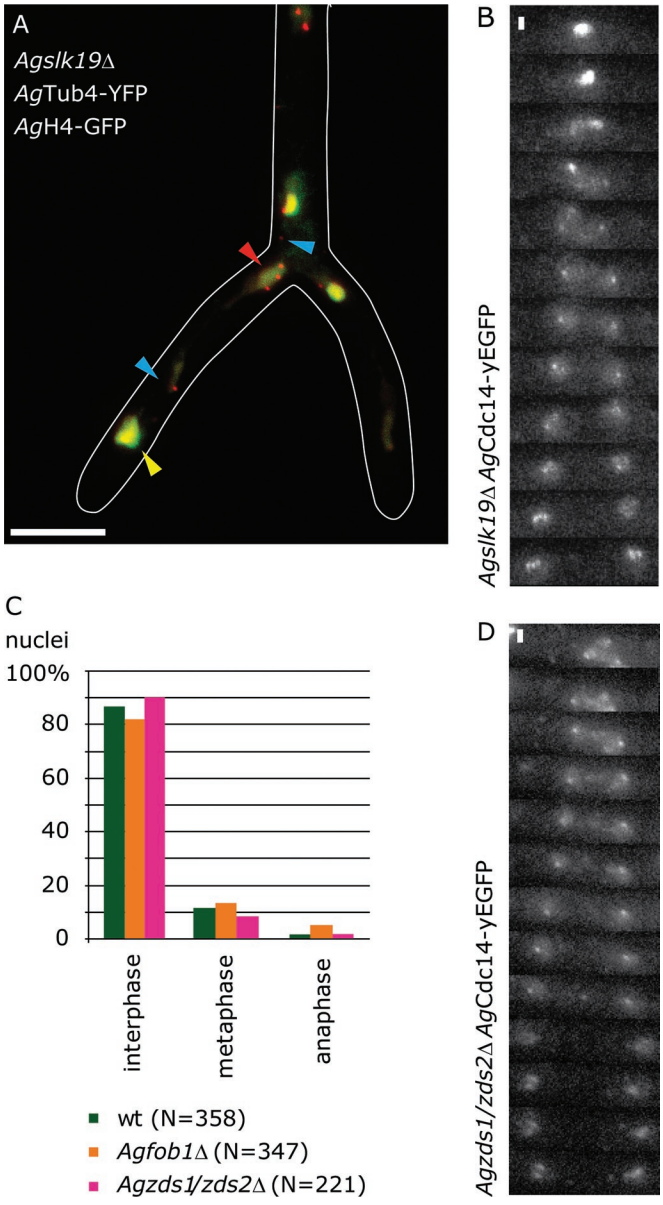

FIGURE 9: Nonlethal FEAR mutants. (A) Channel merge of *Ag*Tub4-YFP (red) and *Ag*H4-GFP (green) images of fast-growing (as indicated by tip splitting) hyphae on TL slides. Yellow arrowhead indicates nucleus with no SPB. Red arrowhead indicates nucleus with three SPBs. Blue arrowheads indicate lone SPBs attached to no nucleus or nuclear fragment. Scale bar, 10 µm. (B) Time lapse series of *Ag*Cdc14-yEGFP in mature *Agslk19*Δ mycelium. Time interval, 1 min. Scale bar, 1 µm. (C) Percentages of total counted nuclei found to be in different nuclear division cycle stages in wild-type reference strain (*Ag*H4-GFP *Ag*Tub4-YFP) and FEAR mutants. (D) Time-lapse series of *Ag*Cdc14-yEGFP in mature *Agzds1/zds2*Δ mycelium. Time interval, 1 min. Scale bar, 1 µm.

phenotype in nuclear division for the null mutants, given the clear effect on *Ag*Cdc14 release and mitosis of the *Agcdc55*Δ deletion and the putative inhibitory function toward PP2A^{AgCdc55} of *Ag*Zds1/Zds2. Although we expected to observe defects in nuclear segregation as in the *Agspo12/bns1*Δ strains, we could not detect any mitotic phenotype of any nature. As it seems, *Ag*Zds1/Zds2 is not involved in PP2A^{AgCdc55} down-regulation. The proposed mechanism for its regulation in budding yeast—controlled partitioning of the phosphatase between cytoplasm and nuclei (Rossio and Yoshida, 2011)—is most likely not appropriate for multiple nuclei containing hyphae. Perhaps in *A. gossypii*, PP2A^{AgCdc55} is directly inhibited by *Ag*Esp1 activity, and the inclusion of the polyvalent *Sc*Zds1 and *Sc*Zds2 (roles have been described in cell polarity, chromatin silencing, chromatid cohesion, and even cell wall integrity signaling) in the FEAR pathway in budding yeast reflects a strategy to time polarity- or cell wall–related events to occur during anaphase, a layer of cross-coordination that *A. gossypii* can do without.

*Ag*Slk19Δ cells displayed disturbed mitosis, leading to a density of nuclei roughly half of that in wild type. Most likely these defects are not due to misregulation of *Ag*Cdc14, as release dynamics was seemingly unaffected in our mutants. Rather, what we observe is possibly the result of a malfunction of separase due to the lack of interaction with *Ag*Slk19. The observations of more than two SPBs on some nuclei are likely due to *Ag*Esp1 triggering *Ag*Cdc14 release and exit from mitosis without properly cleaving cohesin. Multiple SPBs are also observed in budding yeast *esp1-1* cells at the restrictive temperature (McGrew *et al.*, 1992).

*Ag*Cdc14 release depends on a simplified version of the FEAR pathway

The system promoting Cdc14 release has developed differently in the *A. gossypii* lineage than with *S. cerevisiae*. The underlying pathways controlling this pivotal phosphatase are not conserved as such in *A. gossypii*. Homologues of the MEN still apparently function together as a G protein–coupled kinase cascade at the SPBs. This core signaling unit, however, seems to be uncoupled from any function in *Ag*Cdc14 release and exiting mitosis. The module appears to play a crucial role in septation, which also calls to mind the septation initiation network of *Schizosaccharomyces pombe*, which is required for (*Sc*Cdc14 orthologue) *Sp*Clp1-dependent septum formation and is largely made up of MEN homologues.

The FEAR network, on the other hand, seems to be functionally conserved in *A. gossypii*, although in a reduced form. *Ag*Zds1/Zds2 and *Ag*Fob1 have not been shown to play a role in *Ag*Cdc14 release, and *Ag*Slk19 may only be involved as a cofactor in cohesin cleavage but not in FEAR activation. The reduced redundancy within the remaining system seems to be reflected in more drastic phenotypes of deletion mutants than in *S. cerevisiae*: *Ag*Spo12/Bns1 and the putative PP2A regulatory subunit *Ag*Cdc55 have obtained essential status. This is similar to the situation during meiosis I in *S. cerevisiae*, in which FEAR is essential for proper *Sc*Cdc14 release and MEN is not. Meiosis I division notably takes place without ensuing cytokinesis and likely without orientational cues as needed for mitosis.

As to how the regulatory network controlling exit from mitosis in *A. gossypii* may be wired, we propose a stripped-down model (Figure 10).

Concluding remarks

It has been suggested that, in primitive cells, where the orientation of mitosis might be inconsequential, the FEAR network could represent the sole mechanism for Cdc14 release, and that the MEN emerged later, coevolving with oriented cell division (Bosl and Li, 2005). In some ways, *A. gossypii* shares some analogy to such a primitive cell and may well resemble simple primordial organisms taking first steps in cell division. However, in the case of *A. gossypii*, we can presume that ancestors were mononuclear organisms and that the current morphology and lifestyle were attained by the loss of functions once possessed. This derives from the fact that

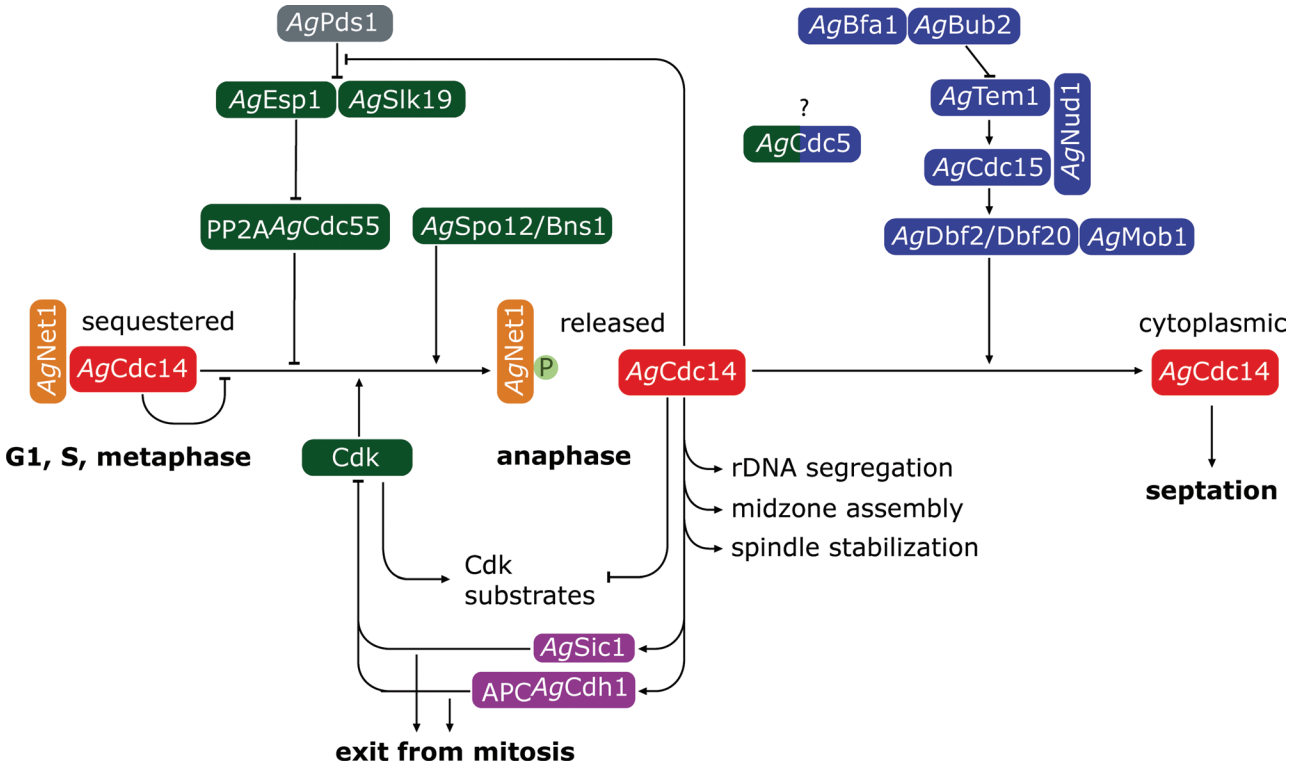

FIGURE 10: Proposed wiring diagram of exit from mitosis homologues in *A. gossypii*; based on *S. cerevisiae* model and minimally reduced by nodes and connections that are suggested to be ruled out by experimental data. Of interest, calculated sequence identity values for all genes in the system are either particularly high (>70%) or rather low (<50%) with no values in between (Supplemental Figure S1). This pattern may indicate points of particularly high evolutionary pressure on the system. To a certain degree high identity values reflect areas of the network map that are likely to be conserved: The only highly conserved FEAR homologues are all part of the putative PP2A^{AgCdc55} phosphatase. Of the MEN, the cascade components *Ag*Tem1, *Ag*Dbf2/Dbf20, and *Ag*Mob1 are strongly conserved. During evolution the cellular function of this signaling group has largely been modified by altering upstream and downstream elements and not the pathway itself.

MEN homologues in several other organisms coordinate cytokinesis with the cell cycle and from studies suggesting that the evolution of septation in *A. gossypii* is also strongly influenced by significant loss of function in the course of evolution (Kaufmann and Philippsen, 2009). In any case, coordination of nuclear division is bound to fewer conditions than in budding yeast, and this is directly reflected in reduced complexity of the regulatory pathways. It is likely that the need for combined circuitry motifs for general signal enhancement or stabilization during mitosis is not the primary cause of the complexity observed in *S. cerevisiae*. The simpler system described in *A. gossypii* may provide grounds for clarifying questions that have been difficult to tackle in *S. cerevisiae*, for example, the precise role of polo kinase Cdc5 in exit from mitosis.

MATERIALS AND METHODS

Strains and plasmids

A. gossypii media and culturing are described in Ayad-Durieux *et al.* (2000) and Wendland *et al.* (2000). *A. gossypii* transformation was performed as described in Wendland *et al.* (2000).

All plasmids and strains used in this study are listed in Supplemental Tables 1 and 2, respectively. Oligonucleotides are listed in Supplemental Table 3 and were synthesized by Microsynth (Balgach, Switzerland). For recombination of plasmids and PCR products, both were cotransformed into the budding yeast host strain DY3 (*MATα his3Δ200 trp1Δ63 leu2Δ1 ura3-52Δ*) according to Gietz *et al.* (1995). Plasmids were isolated from yeast as previously described (Schmitz *et al.*, 2006).

To construct pMF8, the *Ag*NOP1 locus was amplified by high-fidelity PCR from genomic DNA using the primers NOP1*Spe*Iup and NOP1*Bam*HIdown. A *Bam*HI/*Spe*I digest of the product was sticky-end ligated into a *Bam*HI/*Spe*I–digested pRS416 backbone and verified first by enzyme digestion and then by sequencing of the cloned ORF.

pMF12 was constructed by homologous recombination in *S. cerevisiae* cells. pAGT211 was used as a template to generate an insertion cassette with homologous flanking regions using NOP1_F5 and NOP1_F2. The product was cotransformed into DY3 cells together with pMF8, and the resulting fusion plasmid was isolated and verified by enzyme digestion and sequencing of the mCherry moiety and the C-terminus of *Ag*NOP1.

*Ag*Nop1-Cherry *Ag*Cdc14-GFP was generated by transformation and genomic integration of a fragment produced by digestion of pMF12 with *Eco*RI and *Spe*I (and additionally *Dra*I and *Bsp*HI to disrupt autonomously replicating sequence (ARS)-dependent replication of the plasmid). Homokaryons were not functional, so imaging was conducted in heterokaryotic mycelium.

To generate *Ag*Nop1-Cherry *Ag*H4-GFP *Ag*Tub4-YFP, pMF12 was introduced into an *Ag*H4-GFP *Ag*Tub4-YFP background and maintained by constant selection. Genomic integration was not attempted due to the nonfunctionality observed in *Ag*Nop1-Cherry *Ag*Cdc14-GFP homokaryons.

Deletion cassettes for homologous recombination as used for all gene deletions in this article were generated by PCR using pAGT100 (NAT1 marker), pAGT120 (LEU2 marker), or pAGT140 (GEN3 marker) as templates (Kaufmann, 2009) and oligonucleotide primer pairs with 50–base pair homologous flanking sequences for integration. Deletion cassettes were additionally purified prior to transformation by ethanol precipitation or via PCR product purification columns (Roche Diagnostics, Indianapolis, IN).

Construction of the plasmid pMF1 was analogous to that of pMF8 using the primers AgTEM1_CL_Up and AgTEM1_CL_Down. A *Hin*dIII/*Spe*I digest of the product was sticky-end ligated into a pRS416 backbone and verified by enzyme digestion and sequencing. pMF2 was then constructed using pMF1 as a backbone, analogous to pMF12 construction outlined earlier, using AgTEM1_F5 and AgTEM1_F2 and the template pAGT241. The resulting fusion plasmid was isolated from the cotransformed yeast cells and verified by enzyme digestion and sequencing of the yEGFP moiety and the C-terminus of *Ag*TEM1.

pMF3 was constructed in an analogous manner to pMF3, using the plasmid clone of the C-terminus of *Ag*LTE1, pAG7638, as a backbone and the oligonucleotide primers AgLTE1_F5 and AgLTE1_F2 for fusion cassette amplification.

pMF10 was constructed in an analogous manner, using the *Ag*PDS1 clone pAG11556 as a backbone, and pAGT211, combined with the primers PDS_F5 and PDS1_F2, to amplify the mCherry fusion cassette.

A. gossypii strains *Ag*Tem1-GFP and *Ag*Lte1-GFP were generated by transformation and genomic integration of fragments produced by digestion of pMF2 (with *Bss*SI/*Bcl*I) and pMF3 (with *Blp*I), respectively. The *Ag*Pds1-Cherry *Ag*Cdc14-GFP strain was obtained by transforming fragments produced by digesting pMF10 with *Cla*I and *Spe*I (as well as *Xmn*I for ARS disruption). *Ag*Tem1-yEGFP, *Ag*Lte1-yEGFP, and *Ag*Pds1-mCherry were all functional.

Verification of all deletion strains was carried out by analytical PCR, using primer pairs designed to amplify 5′ and 3′ integration boundaries, as well as wild-type (nonintegrated) corresponding regions as controls.

For verification of fluorescent protein fusion transformants generated with plasmid digests, verification PCR primers were designed to amplify 1) the fusion boundary, 2) a nonintegrated region of the plasmid (to be able to rule out a propagation of undigested plasmid leading to resistance toward selective compound), 3) the corresponding N- or C-terminus of the WT allele, and 4) a product indicating integration of the selection marker into the genome.

Selective conditions were maintained with 200 µg/ml Geneticin (G418) disulfate (for GEN3 marker; ForMedium, Hunstanton, United Kingdom), 50 µg/ml clonNAT (for NAT1 marker; Werner BioAgents, Jena, Germany), or leucine dropout minimal medium.

Fluorescence microscopy and image processing

For microscopy, we used an Axioplan2 microscope equipped with the objectives Plan-Apochromat 100×/1.40–numerical aperture oil differential interference contrast (DIC) and Plan-Apochromat 63×/1.40 NA oil DIC (Carl Zeiss AG, Feldbach, Switzerland) and appropriate filters (Zeiss, and Chroma Technology, Brattleboro, VT). The light source for fluorescence microscopy was a Polychrome V monochromator (TILL Photonics, Gräfelfing, Germany). Images were acquired at room temperature using a cooled charge-coupled device CoolSNAP HQ camera (Photometrics, Tucson, AZ) with MetaMorph 6.2r5 software (Molecular Devices, Downingtown, PA). For fluorescence images, multiple planes with a distance between 0.5 and 1 µm in the *Z*-axis were taken. Raw image processing was performed with MetaMorph 6.2r5 software. Z-stacks were optionally deconvolved with the built-in nearest-neighbor algorithm and compressed by maximum or average projection with stack arithmetic and saved as 8-bit grayscale or RGB TIFF files. All measurements were carried out with ImageJ (Wayne Rasband, National Institutes of Health, Bethesda, MD). For in vivo image acquisition, glass slides were prepared covered with 0.6 ml of Ashbya synthetic complete (ASC) or ALF medium (ASC medium with low-fluorescence yeast nitrogen base; Sunrise Scientific Products, San Diego, CA) supplemented with 1% agarose, upon which small pieces of mature mycelium from the border of *A. gossypii* colonies or young mycelia cultured in liquid medium were placed and left to recover for at least 2 h. A total of 30 µl of ASC or ALF was added to mycelium before cells were covered with a coverslip for image acquisition. Chitin (using calcofluor white), and immunofluorescence stainings were performed as previously described (Ayad-Durieux *et al.*, 2000). Rat anti–α-tubulin (YOL1/34; Serotec, Oxford, United Kingdom) was used at a 1:25 dilution and Alexa Fluor 568 goat anti–rat immunoglobulin G (Invitrogen, Carlsbad, CA) at a 1:200 dilution.

Quantification of nuclear division cycle stages

Tip-splitting hyphae were identified on time-lapse (TL) slides, indicating healthy growth, and short (8 min) time-lapse movies were acquired, capturing five planes (1 µm apart) for the *Ag*H4-GFP signal and 13 planes (0.5 µm apart) for the *Ag*TUB4-YFP signal at each time point (1-min time interval). The entire length of the movie was used to determine the category of nuclei in the third time frame, judging by the combined signals from the two channels acquired. Examples of nuclei assigned to different the categories as well as further explanations are shown in Supplemental Figure S2.

*Ag*Cdc14-yEGFP dynamics

Cells harboring *Ag*Pds1-mCherry and *Ag*Cdc14-yEGFP were imaged over 20–30 min, allowing for rare instances in which mitotic events could be entirely followed through. For *Ag*Cdc14-yEGFP measurements, a minimal polygon shape was determined that would engulf the entire area of the yEGFP signal without being altered in size during the course of the series. The intensity of all pixels within this area was measured and the individual values sorted to a histogram of the data. Going back to the raw images, we then calculated intensity means for sample areas within nucleolar foci (for core intensity of sequestered *Ag*Cdc14-yEGFP), within the nucleoplasm of anaphase nuclei (for intensity of released *Ag*Cdc14-yEGFP), and within the hyphae (for brightness of background fluorescence) and used for the other time points later. On the basis of these mean values, borders delimiting these categories were defined. For example, all pixels with intensities greater than a determined value were deemed to represent sequestered *Ag*Cdc14 and could as such be counted. In this manner, counts were determined for each time point for each individual nucleus and plotted against time. These resulting graphs were combined on a common time axis and scaled to correct for artifactual differences in signal intensities and boundary polygon shapes between experiments. *Ag*Pds1-mCherry was treated in an analogous manner but starting with a predefined 80-pixel, large pseudo-circular area placed within the brightest part of the image.

Sequence analysis

Protein alignments were performed with sequences retrieved from the *Ashbya* Genome Database (Gattiker *et al.*, 2007) and the

Saccharomyces Genome Database (Nash *et al.*, 2007). Amino acid sequence identity calculations were performed with the Clone Manager 7 Suite (Scientific and Educational Software, Cary, NC), using default parameters.

ACKNOWLEDGMENTS

We thank Valentin Tilloy, Céline Correia, and Anaïs Sengler for help with strain construction. We are grateful to Frank Uhlmann and Anne Spang for their many helpful suggestions. We especially thank Sandrine Grava for discussions and the *Agbub2*Δ strain. We also acknowledge the help of the Philippsen laboratory, as well as the *A. gossypii* research community. This work was supported by Swiss National Science Foundation Grant 3100A0-112688 (to P.P.).

REFERENCES

Alberti-Segui C, Dietrich F, Altmann-Johl R, Hoepfner D, Philippsen P (2001). Cytoplasmic dynein is required to oppose the force that moves nuclei towards the hyphal tip in the filamentous ascomycete *Ashbya gossypii*. J Cell Sci 114, 975–986.

Ayad-Durieux Y, Knechtle P, Goff S, Dietrich F, Philippsen P (2000). A PAK-like protein kinase is required for maturation of young hyphae and septation in the filamentous ascomycete *Ashbya gossypii*. J Cell Sci 113, 4563–4575.

Bardin AJ, Visintin R, Amon A (2000). A mechanism for coupling exit from mitosis to partitioning of the nucleus. Cell 102, 21–31.

Bosl WJ, Li R (2005). Mitotic-exit control as an evolved complex system. Cell 121, 325–333.

Cohen-Fix O, Peters JM, Kirschner MW, Koshland D (1996). Anaphase initiation in *Saccharomyces cerevisiae* is controlled by the APC-dependent degradation of the anaphase inhibitor Pds1p. Genes Dev 10, 3081–3093.

Corbett M, Xiong Y, Boyne JR, Wright DJ, Munro E, Price C (2006). IQGAP and mitotic exit network (MEN) proteins are required for cytokinesis and re-polarization of the actin cytoskeleton in the budding yeast, *Saccharomyces cerevisiae*. Eur J Cell Biol 85, 1201–1215.

De Wulf P, Montani F, Visintin R (2009). Protein phosphatases take the mitotic stage. Curr Opin Cell Biol 21, 806–815.

Dietrich FS *et al.* (2004). The *Ashbya gossypii* genome as a tool for mapping the ancient *Saccharomyces cerevisiae* genome. Science 304, 304–307.

Gattiker A, Rischatsch R, Demougin P, Voegeli S, Dietrich FS, Philippsen P, Primig M (2007). *Ashbya* Genome Database 3.0: a cross-species genome and transcriptome browser for yeast biologists. BMC Genomics 8, 9.

Gietz RD, Schiestl RH, Willems AR, Woods RA (1995). Studies on the transformation of intact yeast cells by the LiAc/SS-DNA/PEG procedure. Yeast 11, 355–360.

Gladfelter AS, Hungerbuehler AK, Philippsen P (2006). Asynchronous nuclear division cycles in multinucleated cells. J Cell Biol 172, 347–362.

Holt LJ, Krutchinsky AN, Morgan DO (2008). Positive feedback sharpens the anaphase switch. Nature 454, 353–357.

Jin F, Liu H, Liang F, Rizkallah R, Hurt M, Wang Y (2008). Temporal control of the dephosphorylation of Cdk substrates by mitotic exit pathways in budding yeast. Proc Natl Acad Sci USA 105, 16177–16182.

Kaufmann A (2009). A plasmid collection for PCR-based gene targeting in the filamentous ascomycete *Ashbya gossypii*. Fungal Genet Biol 46, 595–603.

Kaufmann A, Philippsen P (2009). Of bars and rings: Hof1-dependent cytokinesis in multiseptated hyphae of *Ashbya gossypii*. Mol Cell Biol 29, 771–783.

Lang C, Grava S, Finlayson M, Trimble R, Philippsen P, Jaspersen SL (2010a). Structural mutants of the spindle pole body cause distinct alteration of cytoplasmic microtubules and nuclear dynamics in multinucleated hyphae. Mol Biol Cell 21, 753–766.

Lang C, Grava S, van den Hoorn T, Trimble R, Philippsen P, Jaspersen SL (2010b). Mobility, microtubule nucleation and structure of microtubule-organizing centers in multinucleated hyphae of *Ashbya gossypii*. Mol Biol Cell 21, 18–28.

Lu Y, Cross FR (2010). Periodic cyclin-Cdk activity entrains an autonomous Cdc14 release oscillator. Cell 141, 268–279.

McGrew JT, Goetsch L, Byers B, Baum P (1992). Requirement for ESP1 in the nuclear division of *Saccharomyces cerevisiae*. Mol Biol Cell 3, 1443–1454.

Meitinger F, Petrova B, Lombardi IM, Bertazzi DT, Hub B, Zentgraf H, Pereira G (2010). Targeted localization of Inn1, Cyk3 and Chs2 by the mitotic-exit network regulates cytokinesis in budding yeast. J Cell Sci 123, 1851–1861.

Mohl DA, Huddleston MJ, Collingwood TS, Annan RS, Deshaies RJ (2009). Dbf2-Mob1 drives relocalization of protein phosphatase Cdc14 to the cytoplasm during exit from mitosis. J Cell Biol 184, 527–539.

Nash R *et al.* (2007). Expanded protein information at SGD: new pages and proteome browser. Nucleic Acids Res 35, D468–D471.

Pereira G, Hofken T, Grindlay J, Manson C, Schiebel E (2000). The Bub2p spindle checkpoint links nuclear migration with mitotic exit. Mol Cell 6, 1–10.

Queralt E, Lehane C, Novak B, Uhlmann F (2006). Downregulation of PP2A(Cdc55) phosphatase by separase initiates mitotic exit in budding yeast. Cell 125, 719–732.

Queralt E, Uhlmann F (2008a). Cdk-counteracting phosphatases unlock mitotic exit. Curr Opin Cell Biol 20, 661–668.

Queralt E, Uhlmann F (2008b). Separase cooperates with Zds1 and Zds2 to activate Cdc14 phosphatase in early anaphase. J Cell Biol 182, 873–883.

Rock JM, Amon A (2009). The FEAR network. Curr Biol 19, R1063–R1068.

Rossio V, Yoshida S (2011). Spatial regulation of Cdc55-PP2A by Zds1/Zds2 controls mitotic entry and mitotic exit in budding yeast. J Cell Biol 193, 445–454.

Schmitz HP, Kaufmann A, Kohli M, Laissue PP, Philippsen P (2006). From function to shape: a novel role of a formin in morphogenesis of the fungus *Ashbya gossypii*. Mol Biol Cell 17, 130–145.

Seshan A, Bardin AJ, Amon A (2002). Control of Lte1 localization by cell polarity determinants and Cdc14. Curr Biol 12, 2098–2110.

Stegmeier F, Huang J, Rahal R, Zmolik J, Moazed D, Amon A (2004). The replication fork block protein Fob1 functions as a negative regulator of the FEAR network. Curr Biol 14, 467–480.

Stegmeier F, Visintin R, Amon A (2002). Separase, polo kinase, the kinetochore protein Slk19, and Spo12 function in a network that controls Cdc14 localization during early anaphase. Cell 108, 207–220.

Sullivan M, Higuchi T, Katis VL, Uhlmann F (2004). Cdc14 phosphatase induces rDNA condensation and resolves cohesin-independent cohesion during budding yeast anaphase. Cell 117, 471–482.

Tomson BN, Rahal R, Reiser V, Monje-Casas F, Mekhail K, Moazed D, Amon A (2009). Regulation of Spo12 phosphorylation and its essential role in the FEAR network. Curr Biol 19, 449–460.

Visintin R, Hwang ES, Amon A (1999). Cfi1 prevents premature exit from mitosis by anchoring Cdc14 in the nucleolus. Nature 398, 818–823.

Wendland J, Ayad-Durieux Y, Knechtle P, Rebischung C, Philippsen P (2000). PCR-based gene targeting in the filamentous fungus *Ashbya gossypii*. Gene 242, 381–391.

Wendland J, Philippsen P (2000). Determination of cell polarity in germinated spores and hyphal tips of the filamentous ascomycete *Ashbya gossypii* requires a rhoGAP homolog. J Cell Sci 113, 1611–1621.

Yoshida S, Asakawa K, Toh-e A (2002). Mitotic exit network controls the localization of Cdc14 to the spindle pole body in *Saccharomyces cerevisiae*. Curr Biol 12, 944–950.